5 cases with PTEN loss harbored KRAS mutations. Strong pAKT expression (grade 2) was seen in 13 cases, 6 (46%) of which were invasive. Interestingly, none of the 5 cases with PTEN loss showed concomitant strong pAKT expression.
Conclusions: PTEN downregulation is less frequent in IPMN than reported in PDAC. PTEN loss appears to be associated with an invasive phenotype, suggesting that it may play a role in neoplastic progression of IPMN. However, PTEN loss is not associated with AKT activation nor KRAS mutations, suggesting an alternative PTEN signaling pathway involved.

1877 Ribonucleotide Reductase M2 Is Not Predictive of Adjuvant Gemcitabine Treatment Benefit in Patients with Resected Pancreatic Adenocarcinoma

H Xie, J Lin, DG Thomas, W Jiang, X Liu. Cleveland Clinic, Cleveland; Indiana University, Indianapolis; University of Michigan, Ann Arbor.
Background: Gemcitabine is used widely as an adjuvant treatment for pancreatic adenocarcinoma. Ribonucleotide reductase small subunit M2 (RRM2), the catalytic subunit of ribonucleotide reductase, is associated with tumor progression and resistance to gemcitabine. Recent studies showed that low mRNA expression of *RRM2*, was predictive of treatment benefit of gemcitabine in patients with resected pancreatic adenocarcinoma (Fujita H et al., Neoplasia 12: 807-17, 2010). This study aims to determine if RRM2 protein expression level assessed by immunohistochemistry is 1) prognostic in patients with resectable pancreatic adenocarcinoma and 2) a predictive marker for treatment benefit of gemcitabine.
Design: 117 patients underwent pancreatic resection for pancreatic adenocarcinoma were included. 44 of them received adjuvant gemcitabine treatment prior to disease recurrence/metastases. Tissue micro-arrays were constructed from paraffin-embedded tumors. RRM2 expression in tumors was determined by immunohistochemistry and grouped as negative or positive. The correlation of RRM2 expression and overall survival (OS) or progression-free survival (PFS) was determined using the Kaplan-Meier method. Cox's proportion hazards multivariate model was also employed to identify prognostic factors.
Results: RRM2 expression showed no prognostic value in the entire group regarding OS (median OS 30.9 vs 13.7 months, p=0.26) and PFS (median OS 20.6 vs 11.8 months, p=0.46). *RRM2* expression was not predictive of OS and PFS in the subgroup of 44 patients who received gemcitabine treatment as an adjuvant therapy either (median OS 31.2 vs 15.2 months, p=0.62; median PFS 11.3 vs 14 months, p=0.35, respectively). Cox's proportion hazards multivariate model showed no prognostic effect of RRM2 expression on OS (HR 0.89, p=0.76) and PFS (HR 1.45, p=0.44) in the subgroup of 44 patients who received gemcitabine therapy. However, the number of positive lymph nodes and perineural invasion are prognostic factor for OS (HR 1.21, p=0.01) and for PFS (HR 5.44, p=0.001), respectively.
Conclusions: RRM2 protein expression level determined by immunohistochemistry on paraffin-embedded pancreatic carcinoma tissue is neither prognostic nor predictive of adjuvant gemcitabine treatment benefit in patients with resectable pancreatic adenocarcinoma.

1878 Low Expression of Ribonucleotide Reductase M1 Predicts Adjuvant Gemcitabine Treatment Benefit in Patients with Resectable Pancreatic Adenocarcinoma

H Xie, W Jiang, J Jiang, Y Wang, R Kim, X Liu. Cleveland Clinic, Cleveland; Veridex LLC, Johnson & Johnson Company, San Diego; Moffitt Cancer Center, Tampa.
Background: Gemcitabine has been a cornerstone of current chemotherapy for pancreatic cancer. Our previous pilot study in 18 patients suggested low expression of *RRM1* was predictive of adjuvant gemcitabine treatment benefit in patients with resectable pancreatic adenocarcinoma (W Jiang et al., Mod Path 23:357A, 2010). This study aims to confirm our previous finding in a larger cohort of patients.
Design: 122 patients underwent pancreatic resection at our institution for resectable pancreatic adenocarcinoma from 10/1999 to 12/2007; 44 of them received adjuvant gemcitabine treatment prior to disease recurrence/metastases. Total RNA was isolated from micro-dissected paraffin-embedded tumors. The expression of *RRM1* in tumors was determined by QRT-PCR and the expression levels were normalized to two endogenous reference genes and stratified into high expression group and low expression group using recursive partitioning analysis. Overall survival (OS) and progression-free survival (PFS) of these two groups were estimated with the Kaplan-Meier method. The prognostic value of *RRM1* expression on OS and PFS was examined with Cox proportion hazards analysis.
Results: *RRM1* expression did not have prognostic value in the entire cohort of patients regarding OS (p=0.14) and PFS (p=0.68). However, in the subgroup of 44 patients who received gemcitabine treatment as an adjuvant therapy, patients with low *RRM1* expression had significantly longer OS (median OS 44.4 vs. 14.5 months; p=0.01, figure A). While Cox proportion hazards multivariate analysis identified number of positive lymph nodes and perineural invasion as predictors of shorter OS (HR 1.18, p=0.02) and shorter PFS (HR 3.5, p=0.004), respectively, it confirmed that low expression of *RRM1* was associated with longer OS (HR 0.35, p=0.009) and PFS (HR 0.37, p=0.004).

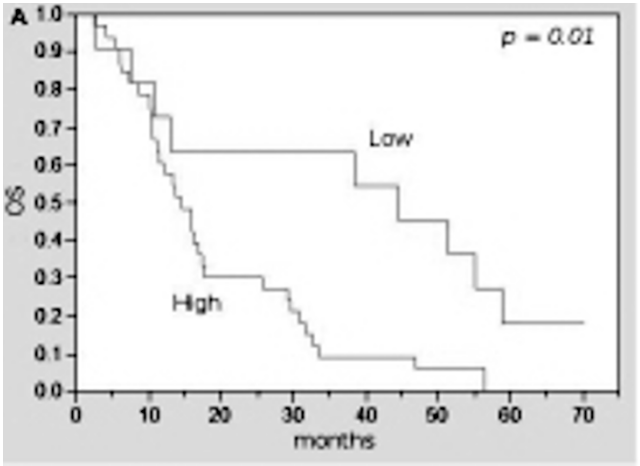

Conclusions: Low *RRM1* expression determined by QRT-PCR on paraffin-embedded pancreatic carcinoma tissue in patients who received gemcitabine as an adjuvant treatment predicts a progression-free and overall survival benefit.

1879 *MDM2* SNP-309 Promoter Polymorphism, MDM2 and p53 Expression in Pancreatic Ductal Adenocarcinoma

X Zhou, J Rock, ME McNally, M Bloomston, W Zhao, G Lozanski, WL Frankel. Ohio State Universcity, Columbus, OH.
Background: The mouse double minute 2 homolog (MDM2) is the primary regulator of p53. A functional single nucleotide polymorphism (SNP) of the *MDM2* promoter (309 T>G) enhances the Sp1 binding to *MDM2* promoter and MDM2 expression resulting in attenuation of p53. Small molecules antagonizing the MDM2-p53 interaction have been shown to promote p53-dependent tumor regression in vitro. The *MDM2* SNP-309 has been recently associated with the development and prognosis of a variety of tumors. We hypothesized that the *MDM2* SNP-309 is associated with increased risk of pancreatic ductal adenocarcinoma (PDAC) and worse outcome.
Design: Genotyping of *MDM2* SNP-309 was performed on genomic DNA extracted from benign lymph node tissue of 189 PDAC by PCR amplification flanking the corresponding promoter region followed by temperature gradient capillary electrophoresis and direct sequencing. Tissue microarrays of PDAC were constructed and immunohistochemically stained for MDM2 and p53. Expression intensity was scored as 0 (absent), 1+ (modest) or 2+ (high). In addition, FISH analysis for *MDM2* amplification was done in 20 PDAC (15 with modest or high expression). We evaluated the association between *MDM2* SNP-309 and the risk of PDAC using Cramer's V Test (with 100 controls). We also investigated the relationships between *MDM2* SNP-309 genotype, MDM2 and p53 expression and tumor stage and survival time.
Results: The *MDM2* SNP-309 genotypes of PDAC were statistically different from those of controls ($P = 0.041$). The frequency of the G allele in PDAC was significantly higher than that in controls ($P = 0.002$).

MDM2 SNP-309 Genotypes in PDAC and Controls

	PDAC (n = 189)	Controls (n = 100)
G/G	31 (16.3%)	12 (12%)
T/G	97 (51.3%)	40 (40%)
T/T	61 (32.1%)	48 (48%)

PDAC, pancreatic ductal adenocarcinoma; P = 0.041

Modest to high levels of MDM2 expression were detected in 56 tumors (29.6%; 1+ in 25, 2+ in 31), and modest to high levels of p53 were detected in 102 (54%; 1+ in 31, 2+ in 71). *MDM2* amplification was not detected in the 20 PDAC analyzed using FISH. No association was observed between *MDM2* SNP-309 genotype, MDM2 and p53 expression level and tumor stage or survival time.
Conclusions: The G allele of *MDM2* SNP-309 is associated with increased risk of PDAC. Modest to high expression levels of MDM2 and p53 are frequently present in PDAC. It is unlikely that *MDM2* SNP-309 or amplification contributes to the high expression level of MDM2. Further investigations with rigorous design are warranted to assess the magnitude of risk of PDAC with *MDM2* SNP-309 and the prognostic value of MDM2 and p53 expression.

Pan-genomic/Pan-proteomic Approaches to Diseases

1880 Identifying Cancer Mutations in Neuroendocrine Prostate Cancer through Massively Parallel DNA-Sequencing of Formalin-Fixed Paraffin Embedded Tissue

H Beltran, K Park, TY MacDonald, R Yelensky, G Frampton, D Lipson, PJ Stephens, MT Cronin, ST Tagawa, DM Nanus, JM Mosquera, MA Rubin. Weill Medical College of Cornell University, New York, NY; Foundation Medicine, Cambridge, MA.
Background: Neuroendocrine prostate cancer (NEPC) is an aggressive lethal variant of prostate cancer that most commonly arises from existing prostate adenocarcinoma (PCa). Despite chemotherapy, most patients survive less than one year. Little is known about the underlying biology of NEPC, as metastases are rarely biopsied. The purpose of this study was to determine the spectrum of somatic mutations in NEPC by using a

novel DNA sequencing platform and to evaluate for targetable molecular alterations.
Design: 44 NEPC and mixed NEPC/PCa were evaluated by study pathologist and 77 high density foci of NEPC, PCa, and benign areas were selected for DNA extraction. Massively parallel sequencing via HiSeq2000 (Illumina, San Diego, CA) was performed using indexed seq libraries constructed by adapter ligation followed by hybridization with optimized capture probes (Agilent, Cupertino, CA). Data was processed using publicly available and newly validated software tools (Foundation Medicine, Cambridge, MA) to make mutation assignments for base alterations, indels and CNAs in 182 cancer associated genes and common sites of rearrangement for 15 genes.
Results: 5/8 biopsies and 62/65 (overall 93%) of prostate foci yielded sufficient DNA (>50 ng) for analysis from 40m of formalin-fixed paraffin embedded tissue (FFPE) tissue. Average median sequence coverage was 934x. *TMPRSS2-ERG* fusion was present in 28% of NEPC. Recurrent homozygous deletions involving *PTEN* and *RB1* were seen, and 1 tumor with *BRCA2* loss. Several high confidence non-synonymous mutations were identified including *TP53* (40%), *CTNNB1* (12%), and less frequently mutations involving *PTEN*, *PIK3CA*, *AR*, as well as other novel mutations/fusions. There was high concordance between NEPC and PCa foci in mixed tumors, as well as between primary tumor and metastases. High confidence lesions were validated with exome sequencing and FISH.
Conclusions: This study shows feasibility of an in-depth DNA analysis using FFPE tissue, and even biopsy material. Comprehensive genome sequencing has nominated novel biologic pathways and provides insight into disease progression from PCa to NEPC, as well as potential new drug targets for a tumor that is currently lethal. This is a useful and comprehensive sequencing tool to evaluate tumors such as NEPC and other metastatic tumors, where obtaining tissue is challenging.

1881 "Calling Cards" Is a Novel Next-Gen Sequencing Approach That Identifies *SRY* Targets

GA Bien-Willner, D Mayhew, R Mitra. Washington University School of Medicine, St. Louis, MO.
Background: SRY is a tissue-specific transcription factor that is necessary and sufficient to drive male sexual determination. While its function as a male-determining factor has been well studied, no mechanism of action for *SRY* has been proven. It has been proposed that *SRY* drives male sexual determination by up-regulating *SOX9*, as well as inhibiting female-specific factors activated by WNT signaling. Interestingly, *SRY* is also expressed in the adult Sertoli cell, implying it has other functions besides sexual development. *SRY* has been postulated to be involved in the formation of gonadoblastomas and sex-cord stromal tumors. Further elucidation of the function of SRY is severely hampered by the fact that no functional antibodies specific to the SRY protein have been produced, precluding chromatin immunoprecipitation (ChIP) or western-blot analysis. Here we present a novel approach to identify protein-DNA interactions and use it to reveal novel SRY binding sites. This technique dubbed "Calling Cards" functions independent of antibodies. Furthermore, it does not rely on freezing DNA-protein interactions and thus can record such interactions over time in cell culture.
Design: The novel "Calling Cards" technique employs a transposase tethered to a transcription factor of interest to insert a marked transposon into the genome at the site of DNA-protein interaction. A *SRY*-transposase construct was created and transfected into mouse ES cells and primary human ovarian cultures enriched for granulosa cells (the female counterpart to the Sertoli cell), marking sites of interaction. The locations of genomic insertions were mapped using massively-parallel sequencing and clusters of SRY-directed insertions were identified.
Results: Using the "Calling Cards" technique, significant *SRY* peaks were found in the 5' and 3' UTR regions of several spermatogenesis-related genes including *Rnf168, Hormad2, Sox11*, and *Bnc2*. Over 5,000 unique insertions were identified throughout the genome per experiment.
Conclusions: The "Calling Cards" technique is a novel way of identifying protein-DNA interactions independent of antibodies. Using this method, we uncovered several previously unknown targets of SRY, suggesting a role in spermatogenesis in the adult testis. Finding genes in this pathway may serve as targets for therapy in mixed germ cell and/or sex-cord stromal tumors.

1882 Mass Spectrometry-Based Glycoproteomic Profiling Identifies SIRP alpa as a Potential Protein Biomarker in Primary Mediastinal Large B-Cell Lymphoma

NA Brown, D Rolland, D Fermin, V Basrur, D Thomas, F Keyoumarsi, K Conlon, KSJ Elenitoba-Johnson, MS Lim. University of Michigan, Ann Arbor, MI.
Background: Primary mediastinal large B-cell lymphoma (PMBCL) is currently recognized as a non-Hodgkin B-cell lymphoma with pathologic, clinical and molecular characteristics which are distinct from other diffuse large B-cell lymphomas (DLBCL) and from classical Hodgkin lymphoma (cHL). However, overlapping histologic and immunophenotypic features of these lymphomas make this diagnostic distinction challenging in some cases. Since a majority of N-linked glycoproteins are either localized on the membrane or secreted, these proteins are attractive targets for the identification of biomarkers that could aid in the distinction of these three lymphomas.
Design: Using a proteomic strategy targeting N-linked glycosylated proteins, we characterized the glycoproteomic profiles of PMBCL, DLBCL, and cHL. Cell lines derived from PMLBL (K1106 and MEDB1), DLBCL (OCILY2), and cHL (L428, L1236 and KMH2) were used for solid-phase extraction of N-linked glycopeptides which were identified and quantified using liquid chromatography and tandem mass spectrometry. A protein selectively expressed in PMBCL was selected for validation using immunohistochemistry of tissue microarrays constructed from 27 cases of PMBCL, 70 DLBCL and 120 cHL.
Results: Glycopeptides from over 250 proteins were identified from each cell line using false discovery rate of < 4.5 %. Over 90% of the peptides contained the NXST motif which identifies distinct sites of asparagines glycosylation. Importantly, mass spectrometry data correlated strongly with known proteins expressed by cHL (CD30) and PMBCL/DLBCL (CD18, CD19, CD22, CD45, CD79A, and CD79B). In addition, a novel glycoprotein signal regulatory protein alpha (SIRP alpha) was found to be selectively expressed by PMBCL. SIRP alpha is a transmembrane signaling protein expressed in monocytes, dendritic cells and granulocytes. Binding to its ligand (CD47) results in negative regulation of leukocyte adhesion and transmigration, macrophage fusion, phagocytosis. Immunohistochemical analysis of tissue microarrays using a monoclonal antibody for SIRP alpha demonstrated expression in 55.6% of PMBCL compared to 22.9% of DLBCL ($p<0.01$) and 6.7% of cHL ($p<0.0001$).
Conclusions: We characterized the glycoproteomics signature of PMBCL, DLBCL or cHL using mass spectrometry. In doing so, we identified a potential biomarker more commonly expressed in PMBCL than in either DLBCL or cHL. This study demonstrates that mass spectrometry-based glycoproteomic profiling can be used for discovery of novel biomarkers and phenotypic profiling.

1883 Backward Chaining Rule Induction Using Multiple Genomic Data Types To Understand Gene Interactions in Ovarian Cancer

SC Chekuri, ME Edgerton. UT MD Anderson Cancer Center, Houston, TX.
Background: Ovarian serous cystadenocarcinomas (OvSC) are the largest malignant tumor category of ovarian cancer. We worked to derive molecular mechanisms relevant to survivalin OvSC using multiple genomic data types as input.
Design: We used mRNA, methylation, and microRNA data for 456 OvCA samples from the cancer genome atlas project (TCGA). Patients were divided into 2/3 training (304) and 1/3 test sets (152) with similar survival distribution. An additional external validation dataset was constructed using 118 samples from a separately published research study. mRNA was normalized using Combat and Robust Multichip Analysis (RMA). A set of genes was identified using supervised principal component analysis (SPCA) to separate high and low survival groups in the training data based on Cox scores. Rank normalized hierarchical clustering (RNHC) was performed on these selected genes to generate two patient clusters. Kaplan Meier (KM) analysis was performed to evaluate significance of separation of survival for the two patient clusters in the test sets. Two genes with the highest Cox scores were selected for network analysis using Backward Chaining Rule Induction (BCRI) with mRNA, methylation status, and miRNA as inputs.
Results: KM results for separable patient clusters using 15 genes identified in the training set were significant in the TCGA test data ($p=0.0033$) and nearly significant in the external test data ($p=0.0601$). BCRI results for the top two genes based on Cox scores demonstrated a combination of methylation status and gene expression in networks generated for the high and low survival groups. Network genes consist of multiple DNA processing and G-coupled receptors including HHEX, RNF113A, DCI with methylation status for EDNRB, HIST1H2BC.
Conclusions: OvSC is a complex disease. BCRI is a methodology that allows the simultaneous evaluation of gene expression along with methylation status and miRNA expression. BCRI has potential to help us understand complex interactions of gene expression and regulation that combine to effect aggressive behavior in ovarian cancer. Genes that function to process mRNA and that effect G-coupled signaling networks appear to be important in ovarian serous adenocarcinoma.

1884 Understanding the Immunopathogenesis of Sarcoidosis through Gene Expression Profiling

C Curtiss, G Christophi, S Landas. SUNY Upstate Medical University, Syracuse, NY; Washington University in St. Louis, St. Louis, MO.
Background: Sarcoidosis is a multisystemic, granulomatous disease of unresolved pathogenesis with broad, variable clinical features. While several environmental agents have been proposed as potential disease triggers, the lack of a single proven etiologic agent suggests that the affected patients may mount an aberrant immune response to various environmental triggers, which result in sarcoidosis. The role of inflammatory cytokine pathways in sarcoidosis pathogenesis has also been suggested by the elevation of inflammatory cytokine profiles in previous studies.
Design: A retrospective review of archived pathology specimens and confirmation of diagnosis of sarcoid granulomas, infectious granulomas, suture granulomas, and normal (non-granulomatous) lung tissue was performed. Formalin-fixed paraffin-embedded (FFPE) tissue was used to isolate mRNA followed by gene-specific quantitative real time RT-PCR using a modified method that accounted for RNA fragmentation. The expression of several genes including cytokines, signaling modulators, chemokines, proteolytic and oxidative enzymes, and adhesion molecules were quantified.
Results: Forty total cases were analyzed and consisted of 13 sarcoid granulomas, 7 infectious granulomas, 8 suture granulomas, and 12 normal lung specimens.We successfully amplified expression of several genes and many of those genes were differentially regulated among sarcoid granulomas and normal lymph nodes or suture granulomas. These genes included the cytokines IFN-γ and IL-12, the chemokines IP-10 and RANTES, and inducible nitric oxide synthase while housekeeping genes like GAPDH and actin were expressed in similar amounts in all tissues.
Conclusions: Our study demonstrated that it is feasible to use FFPE specimens of granulomatous inflammation and normal tissue to assess gene expression via quantitative real time RT-PCR. Furthermore, preliminary results suggest that specific genes are differentially regulated in sarcoid granulomas, which might provide new molecular or immunohistopathologic diagnostic avenues.

1885 A Target Capture Based Next Generation Sequencing Panel for Identification of Reurrent Somatic Mutations in Cancer

E Duncavage, D Spencer, H Abel, S Kulkarni, K Seibert, R Nagarajan, R Mitra, M Watson, J Pfeifer. Washington University, St. Louis, MO; Washington University, St Louis, MO.

Background: The detection of recurrent somatic mutations in cancer has become increasingly important to both the diagnosis and treatment of many malignancies. Current molecular testing paradigms rely on disparate methods to detect underlying sequencing alterations one gene at a time. Next Generation Sequencing (NGS) allows for the comprehensive sequencing of whole genomes at low cost, however these methods are generally optimized for the discovery of constitutional single nucleotide variation (SNV). Here we demonstrate that NGS can be used to detect a spectrum of clinically-relevant DNA mutations, including SNVs, insertions/deletions (indels), gene amplification, and translocations.

Design: We identified a set of cases with known recurrent somatic mutations including SNVs (10 cases), insertions (11), deletions (1), gene amplifications (3), and translocations (1). Genomic DNA was extracted from formalin-fixed or fresh tissue, indexed sequencing libraries created, and DNA captured using a set of custom-designed cDNA capture probes targeting a 437kb region including 28 genes commonly mutated in cancer. Cases were sequenced in multiplex using 2x101bp reads and the resulting data aligned to the human genome. SNVs were identified using the freely available Genome Analysis Toolkit and indels were identified using Pindel. Translocations were identified using Breakdancer and Slope.

Results: Each case generated approximately 12 million reads, resulting in a mean capture region coverage of 3076x, with a 47% on-target reads. Using well-characterized HapMap DNA we estimated a SNV sensitivity of >99% for heterozygous alleles; for alleles present at 10% frequency, the sensitivity was 98% with a positive predictive value of 94%. Using multiple software packages we identified somatic SNVs in 10 of 10 tested cases, *FLT3* insertions in 10/11 cases, *KIT* deletions in 1/1 cases, *EGFR* gene amplifications in 3/3 cases, and *MLL* translocations in 1/1 case.

Conclusions: We demonstrate that high-coverage, targeted NGS is well-suited for the identification of the full spectrum of somatic mutations present in cancer. Further, we show that targeted NGS can reliably detect mutations present at 10% allele frequency, allowing for the detection of mutations in dilute tumor populations. As the number and complexity of recurrent cancer mutations increases, NGS-based methods will undoubtedly become invaluable in the clinical laboratory.

1886 Identification of Heterogeneous Nuclear Ribonucleoprotein K (hnRNP K) as a Biomarker in Hepatocellular Carcinoma in Patients with Cirrhosis by Proteomic and Immunohistochemical Studies

Y Guo, J Zhao, J Bi, M Chen. Beijing Jishuitan Hospital, Beijing University Health Science Center, Beijing, China; University of California Davis Medical Center, Sacramento, CA.

Background: Hepatocellular carcinoma (HCC), one of the most common malignant tumors worldwide, is particularly prevalent in Asian countries. Hepatitis B (HBV) and Hepatitis C (HCV)-associated cirrhosis are the major common risk factors of HCC. The diagnosis of HCC in a background of cirrhosis can be challenging. In this study, the biomarkers to distinguish HCC from cirrhotic nodules were studied.

Design: Frozen samples from 40 HBV-associated post-operative HCC patients and the clinicopathological data were collected. We used two-dimensional gel electrophoresis(2-DE) coupled with tandem mass spectrometry (MS) to study the proteins differentially expressed in HCC and the adjacent non-HCC cirrhotic tissue. Furthermore, the correlations between potential biomarkers and clinicopathological data of HCC were evaluated using bivariate correlation analysis.

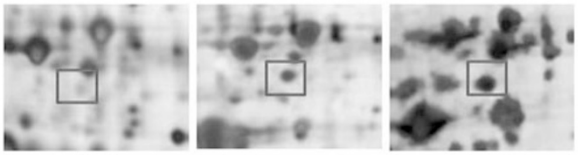

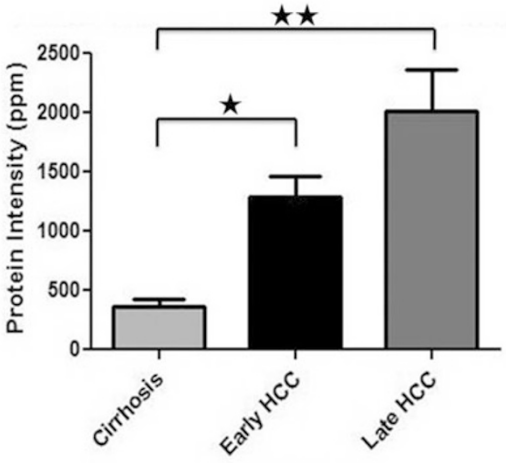

Results: Heterogeneous nuclear ribonucleoprotein K (hnRNP K) was markedly upregulated in HCC compared to the non-HCC cirrhotic tissue. The overexpression of hnRNP K in HCC tissues was further confirmed by Western blot and immunohistochemistry. Receiver operating characteristic (ROC) curve analysis revealed that hnRNP K in combination with serum AFP was a sensitive (93.3%) and specific (96.0%) marker to detect HCC in HBV infected cirrhotic liver tissues.

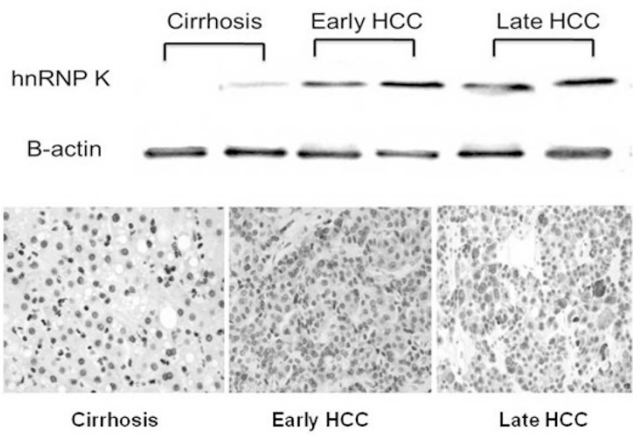

Conclusions: The study revealed overexpression of hnRNP K in HCC which could be a potential diagnostic marker and a candidate target for therapy.

1887 Global 5-Hydroxymethylcytosine Content Is Significantly Reduced in Human Cancers

MC Haffner, A Chaux, AK Meeker, DM Esopi, J Gerber, LG Pellakuru, A Toubaji, P Argani, C Iacobuzio-Donahue, WG Nelson, GJ Netto, AM De Marzo, S Yegnasubramanian. Johns Hopkins University, Baltimore, MD.

Background: DNA methylation at the 5-position of cytosines (5mC) represents an important epigenetic modification involved in tissue differentiation and is frequently altered in cancer. Recent evidence suggests that 5mC can be converted to 5-hydroxymethylcytosine (5hmC) in an enzymatic process involving members of the TET protein family. Such 5hmC modifications are known to be prevalent in DNA of embryonic stem cells and in the brain, but the distribution of 5hmC in normal and neoplastic tissues has not been rigorously explored.

Design: We developed a robust immunohistochemical detection method to evaluate global 5hmC in formalin fixed paraffin embedded tissues. This technique was used to study the distribution of 5hmC in a large set of normal tissues, pre-invasive lesions and invasive carcinoma.

Results: We found that 5hmC was abundant in the majority of normal adult tissues. Interestingly, 5hmC appeared to track with differentiation in hierarchically organized tissues, with less differentiated cell compartments showing lower 5hmC staining. We furthermore noted a strong difference in 5hmC levels between normal and neoplastic tissues. Pre-invasive lesions showed a significant reduction of 5hmC levels. 5hmC content was further profoundly decreased in invasive carcinoma of the prostate, colon and breast.

Conclusions: Our findings suggest a distinct role for 5hmC in tissue differentiation, and furthermore provide first evidence for its loss in pre-invasive lesions and invasive carcinoma. We therefore hypothesize that alterations of 5hmC might be intimately associated with malignant transformation and could be an early event in tumor progression.

1888 Multisite Analytical Validation of a 92-Gene Molecular Classifier for Cancers of Uncertain Primary

SE Kerr, CA Schnabel, PS Sullivan, Y Zhang, V Singh, B Carey, MG Erlander, WE Highsmith, SM Dry, EF Brachtel. Mayo Clinic, Rochester, MN; bioTheranostics, Inc., San Diego, CA; University of California Los Angeles, Los Angeles, CA; Massachusetts General Hospital, Boston, MA.

Background: With increasing use of site- and subtype-specific cancer therapies, accurate tumor classification is of paramount importance to optimize treatment and improve patient outcomes. Diagnosis remains uncertain in 2-5% of solid malignancies after standard histopathologic evaluation. Gene expression-based molecular classifiers have been proposed as a diagnostic aid. This study evaluates the performance of a 92-gene molecular classifier (CancerTYPE ID, bioTheranostics Inc.) for identification of tumor type and subtype in a large multi-institution cohort.

Design: Formalin-fixed paraffin-embedded tumors representing 28 tumor types and 50 subtypes predicted by the molecular classifier were selected and passed pathologist-adjudicated review at 3 institutions. Blinded tumor sections were submitted and tested using a prespecified classification model that reports computational algorithm results as rank probabilities. The top-ranking tumor type predicted by the classifier was compared to the adjudicated reference diagnosis.

Results: The study cohort was comprised of 790 tumors with at least 25 and 10 cases for each classifier type and subtype, respectively. Forty-seven (5.9%) cases were considered unclassified by the assay. The overall concordance rate of the assay prediction with the reference diagnosis was 87% at the main type level and 82% at the subtype level. The reference diagnosis was within the top two rank predicted types in 91% of cases. No statistically significant differences in performance were observed in subset analyses of primary versus metastatic tumors, by grade, or by biopsy type.

Performance by Tumor Type

Type	Concordance %	Type	Concordance %
Adrenal	96	Melanoma	88
Brain	96	Meningioma	100
Breast	80	Mesothelioma	87
Cervix-adeno	72	Neuroendocrine	98
Endometrium	48	Ovary	86
Gastroesophageal	65	Pancreatobiliary	88
GIST	92	Prostate	100
Germ-cell	83	Sarcoma	95
HeadNeck-salivary	88	Sex-cord-stromal	80
Intestine	85	Skin-basal-cell	100
Kidney	97	Squamous	86
Liver	96	Thymus	72
Lung	65	Thyroid	96
Lymphoma	84	UrinaryBladder	64

Conclusions: The 92-gene assay demonstrated excellent overall performance for classification of a diverse set of tumor histologies. Variable positive predictive values indicate that the classifier may be more useful for some differential diagnoses than others. Results from this large scale validation study support the clinical utility of the 92-gene assay as a standardized adjunct to clinicopathologic findings.

1889 Renal Cell Tumors Share Common Type-Specific Copy Number Variations Identified Via SNP Arrays and Whole Genome Sequencing

WA LaFramboise, SI Bastacky, AV Parwani, R Dhir. University of Pittsburgh, Pittsburgh, PA.

Background: Annual renal cell carcinoma (RCC) cases have increased steadily in the United States for 3 decades with diagnosis complicated by overlapping RCC tumor subclassifications. Differential diagnosis relies largely on morphological and immunohistochemical analysis of tissue specimens.

Design: Copy number variant (CNV) analysis was performed on 5 to 7 prototypical renal cell carcinoma (RCC) specimens per tumor classification (chromophobe, clear cell, oncocytoma, papillary 1, papillary 2) using high resolution SNP arrays (1.85 million probes) for comparison to a SNP database of 31 normal tissues created in our laboratory. Two additional papillary 2 specimens (blood and tumor) were subjected to post-hoc array analysis and whole genome sequencing using massively parallel next generation sequencing (Life Technologies: SOLiD4 platform).

Results: RCC samples exhibited diverse genomic changes within and across tumor types ranging from 106 CNV segments in a clear cell specimen to 2238 CNV segments in a papillary type 2 specimen. Despite the genomic heterogeneity, distinct CNV segments were common within each of 4 tumor classifications: chromophobe (7 segments), clear cell (3 segments), oncocytoma (9 segments), and papillary type 2 (2 segments). Shared segments ranged from a 6.1 Kb deletion among oncocytomas to a 208.3 Kb deletion common to chromophobes. Among common tumor type-specific variations, chromophobe, clear cell and oncocytomas comprised exclusively non-coding DNA. No CNV regions were common to papillary 1 specimens although there were 12 amplifications and 12 deletions in 5 of 6 samples. Three microRNAs and 12 mRNA genes had ≥ 98% of their coding region contained within CNV regions including multiple gene families (chromophobe: amylase 1A, 1B, 1C; oncocytoma: general transcription factor 2H2, 2B, 2C, 2D). Gene deletions involved in histone modification and chromatin remodeling affected individual subtypes (clear cell: SFMBT, SETD2; papillary 2: BAZ1A) as well as the collective RCC group (KDM4C). Fine mapping of chromosomes 9 and 14 using whole genome sequencing identified deletions in two regions (9p24.1, 14q13.2) concordant with changes identified in all papillary 2 specimens using SNP arrays.

Conclusions: The finding that 4 of 5 subclassifications of renal neoplasms shared common copy number variants was unexpected given the prevailing theory that cancers arise from disparate genomic changes that induce tumorigenesis. The genomic amplifications/deletions identified in each renal tumor type represent potential diagnostic and/or prognostic biomarkers.

1890 Chromosome Complexity Is Associated with Age and Metastasis in Synovial Sarcomas: Validation of Expression and Genomic Prognostic Signatures

P Lagarde, J Przybyl, C Brulard, A Italiano, D Orbach, B Bui, P Terrier, R Sciot, M Debiec-Rychter, J-M Coindre, F Chibon. Bergonie Institute, Bordeaux, France; INSERM U916, Bordeaux, France; Curie Institute, Paris, France; IGR, Villejuif, France; Catholic University and University Hospitals, Leuven, Belgium.

Background: Synovial sarcoma (SS) is a high grade soft tissue sarcoma which accounts for 2-5% of all soft tissue sarcomas. It is one of the rare sarcomas that occur in adolescents as well as in adults. Nevertheless, metastasis occurs with a much lower frequency in the former. SS oncogenesis is explained by a specific translocation t(X;18), but the genetic basis of SS metastasis is poorly understood. We recently published expression (CINSARC) and genomic (GI) prognostic signatures related to mitosis control and chromosome integrity in other sarcomas and asked whether these signatures could predict SS outcome.

Design: We selected fully annotated primary untreated SS with frozen tissue and molecular confirmation. We established expression and genomic profiles for 92 and 79 SS cases, respectively.

Results: As demonstrated by metastasis-free survival and multivariate analyses, CINSARC and GI have strong and independent prognostic values ($p < 1 \times 10^{-4}$). To identify a SS specific signature, we compared expression profiles of SS with or without metastasis in a training set and a 52-genes prognostic signature was identified and validated in a validation set. These genes are involved in the same pathways than CINSARC and 14 are common with CINSARC.

Moreover, comparing genomic profiles of adult *versus* pediatric SS we observed that in both situations metastasis was associated with genome complexity and that the adult genome was much more frequently rearranged. In line with this, the pediatric good-prognosis patients, according to GI, do not metastasize.

Conclusions: Results clearly indicate that SS metastasis development is associated with chromosome complexity and mitosis control and that CINSARC and GI are powerful prognostic factors. Data also mean that the higher metastasis frequency in adult SS likely is associated to the higher frequency of rearranged genome in adults.

Finally, among these signatures, GI is the best overall and clearly the most clinically relevant considering that CGH is applicable to FFPE samples and already used in pathology laboratories. We now aim to set up a clinical trial to validate GI as eligibility criteria for chemotherapy, specifically in pediatric SS.

1891 Assessment of CGH-Array Usefulness in Metachronous Tumors

F Le Loarer, P Lagarde, A Neuville, JM Coindre, F Chibon. Rouen University Hospital, Rouen, France; Institut Bergonié, Bordeaux, France.

Background: Poorly differentiated metachronous tumors challenge pathologists ability to distinguish confidently a recurrence of the first tumor from a distinct tumor event. Traditional approach is based upon conventional morphology supplemented by immunohistochemistry. The use of molecular tools on a routine basis has long been hindered by the requirement of frozen material. CGH-array protocols have been recently adapted to comply with formalin-fixed paraffin-embedded (FFPE) material. We assessed CGH array technical feasability and diagnostic utility in a series of metachronous tumors.

Design: We selected seven consecutive cases of metachronous malignancies submitted for expert review from December 2010 to April 2011. In all cases, the second event was a poorly differentiated sarcomatoid malignant tumor. CGH-array was performed on Agilent platform with 60k oligo-array. The molecular biologist compared blindly the genomic profiles of couples of metachronous tumors to render a diagnosis of recurrence of the first tumor or distinct tumor events.

Results: Two out of seven cases provided poor quality genomic DNA precluding confident CGH analysis. Technical limitations were due to cellularity of one specimen and poor quality fixation step in the other one. Apart these limitations, we reached high quality CGH-array analysis equivalent to frozen sample-based analysis. Genomic-based diagnoses were in accordance with morphology in three cases out of five and contradicted morphology in one case. No definitive genomic diagnosis could be rendered in one case.

Cases review

Gender - Age*	Primary site	Date of primary	Diagnosis of primary	Second site	Histologic diagnosis	Genomic analysis
female 63	maxilla	2010	sarcomatoid carcinoma	adrenal gland	metastasis	same tumor
male 56	kidney	2000	clear cell carcinoma	maxilla	pleomorphic sarcoma	distinct tumor
male 70	tongue	2004	squamous carcinoma	gengiva	recurrence of carcinoma	distinct tumor
female 61	meninges	2007	meningioma	adrenal gland	metastasis	same tumor
male 69	cervical lymph node	2008	squamous carcinoma	breast	metastasis	NA
female 68	kidney	2008	papillary carcinoma	humerus	metastasis	NA
male 76	kidney	2007	papillary carcinoma	liver	metastasis	uncertain

* age at the primary

Conclusions: According to our results, CGH-array can be fully applied to FFPE material. The technical caveats we met were due to fixation step and cellularity of the sample, emphasizing the need for pre-analytic step standardization. A larger scale use of CGH-array would require further reflection upon the appropriate manner to analyse genomic profiles. We are committed to assess this issue on a larger series.

1892 Rr-1, a Novel Ribosomal RNA-Derived Small Non-Coding RNA, Is Involved in Renal Cell Carcinoma Metastasis

Y Li, X Wu, H Gao, C Guo, JM Jin, F Wang, B Mu, X Li, J Wang, M D'Apuzzo, LM Weiss, H Wu. City of Hope National Medical Center and Beckman Research Institute, Duarte, CA; Third Military Medical University, Chongqing, China.

Background: Small non-coding RNAs (smRNAs) are involved in almost every biological process. SmRNAs that are involved in RNA interference (RNAi) are characteristically associated with Argonaut family proteins and function as the core of RNA-induced silencing complex (RISC). Some smRNAs have been reported to be derived from tRNAs, snoRNAs and introns. By deep sequencing of Ago2-bound small RNA fragments in renal cell carcinoma (RCC) cell lines, we have found a group of smRNAs to be derived from tRNAs, rRNAs, snoRNAs, snRNAs, scRNAs, Mt-tRNAs, introns and exons. We have also found many of them to be Dicer-associated and to be differentially expressed in localized and metastatic RCCs. Here, we report the study to characterize Rr-1, an rRNA-derived smRNA (rd-smRNA), in RCC metastasis.

Design: (1) Explore the structure of Rr-1 and its potential immediate precursor in rRNA by bioinformatics and laboratory studies. (2) Examine and validate Rr-1 differential expression in benign kidney tissue, localized and metastatic RCCs in an RCC frozen tissue cohort (n=24) using our whole genome smRNA deep sequencing data. (3) Characterize the function of Rr-1 on cell proliferation, migration and invasion by knocking down Rr-1 expression in ACHN, a metastatic RCC-derived cell line. (4) Investigate Rr-1-associated pathways by whole genome mRNA deep sequencing of Rr-1 knockdown metastatic RCC cells.

Results: (1) Rr-1 is found to be derived from 18S rRNA which harbors the potential Rr-1 immediate precursor in one of its stem loop structure. (2) Rr-1 is differentially expressed in benign kidney tissue, localized and metastatic RCCs. (3) Knockdown of Rr-1 significantly inhibits the cell proliferation, migration and invasion in metastatic RCC cells. (4) Knockdown of Rr-1 affects expression of a group of genes involved in cell cycle-related pathways.

Conclusions: We are the fist to report that Rr-1, a novel rd-smRNA, is involved in RCC metastasis by affecting metastatic tumor cell proliferation, migration and invasion through cell cycle-related pathways. This finding broadens our view of the function of smRNA and rRNA in tumorigenesis and metastasis.

1893 Piwi-Interacting RNAs Are Differentially Expressed in Renal Cell Carcinoma and Its Metastasis

Y Li, X Wu, H Gao, X Li, JM Jin, F Wang, B Mu, J Wang, YS Kim, LM Weiss, H Wu. City of Hope National Medical Center and Beckman Research Institute, Duarte, CA; Third Military Medical University, Chongqing, China.

Background: Piwi-interacting RNAs (piRNAs) are a distinct group of abundant small non-coding RNAs (smRNAs) of ~24-30 nucleotides in length. They form the piRNA-induced silencing complex (piRISC) with Piwi family proteins in the germ line across animal species and protect genome integrity by transposable elements (TEs) silencing. Owing to their limited expression in gonads and sequence diversity, piRNAs remain the most mysterious class of smRNAs. Recent pilot studies have shown that piRNAs are present in somatic tissues including some human cancers. However, the functional significance of piRNA in somatic cells or human cancers is still not clear. Here, we report the study to profile piRNA expression in renal cell carcinoma (RCC) and its metastasis.

Design: Using a publically available piRNA database (RNAdb: http://Research.imb.uq.edu.au/), we investigated whether piRNAs are present in our whole genome smRNA deep sequencing data from an RCC tissue cohort including benign kidney tissue, localized and metastatic RCC specimens (n = 24). Using the same tissue cohort, we profiled the piRNA expression between benign kidney tissue and RCCs. We further characterized the piRNA differential expression in localized and metastatic RCCs.

Results: (1) 530 piRNAs have been found to be present in at least 3 out of 24 tissue specimens (≥10 copies/reads in at least 1 specimen). (2) 80 piRNAs have been found to be dysregulated in tumors (≥1-log2 ratio, $p < 0.05$), including 19 up-regulated and 61 down-regulated. (3) 34 piRNAs have been found to be dysregulated (all up-regulated) in metastatic RCCs compared to the localized ones (≥1-log2 ratio, $p < 0.05$).

Conclusions: We are the first to show that piRNAs are present in benign and malignant kidney tissues. We have shown the altered expression of piRNAs in RCCs compared to their benign counterparts. We have further characterized the differential expression of piRNAs in localized and metastatic RCCs. These findings may indicate the biological significance of piRNAs in tumorigenesis and metastasis.

1894 Genomic Landscape of Bladder Cancer Development from Incipient Field Effects to Invasive Disease

T Majewski, J Bondaruk, S Zhang, S Lee, K Baggerly, C Dinney, HB Grossman, XF Wu, J-P Issa, W Zhang, R Gibbs, SE Scherer, BA Czerniak. UT MD Anderson Cancer Center, Houston, TX; Fels Institute for Cancer Research and Molecular Biology, Philadelphia, PA; Baylor College of Medicine, Houston, TX.

Background: We are pursuing a unique strategy to identify early events in bladder cancer development by the genome-wide analysis of somatic changes in tissues from resected bladders and characterized pathologically as transitional cell carcinoma. We then extend this analysis into precursor intraurothelial lesions and normal urothelium in the context of the entire organ descriptively referred to as whole-organ histologic and genetic mapping.

Design: Data was derived from 12 tumor-peripheral blood normal pairs to identify somatic variants using NimbleGen whole exome capture with Illumina HiSeq 2000 exome sequencing (20x coverage) and whole genome sequencing (4x coverage) complemented with custom genotyping using Illumina HumanOmni2.5_8 chips. All somatic mutations were tested geographically across the bladder using semi-automated PCR-based sequencing to generate whole-organ maps of bladder cancer development from *in situ* field effects. These results are being augmented by epigenomic and transcriptome analyses using Illumina chips.

Results: Variant analysis, after filtering, revealed that more than 70% of the somatic changes present across the samples were classified as novel and included nearly 4000 missense and approximately 100 nonsense mutations as well as several frame shift alterations. Preliminary analysis revealed mutations in the RAS-ERK MAPK signaling pathway in the early *in situ* phase of bladder carcinogenesis and the involvement of the p53 gene network in the progression from carcinoma *in situ* to invasive cancer.

Conclusions: Genome variant analysis in the entire bladder mucosa revealed complex genomic alterations engaged in the development of diffused mucosal field effects with predominant involvement of the Ras-ERK related genes. The hallmark of the secondary clonal evolution into carcinoma in situ progressing to invasive disease was the alterations of the p53 gene network.

1895 Downregulation of Genes Contributes to Chemoresistance Induced by Hypoxia

LM McEvoy, SA O'Toole, CD Spillane, CM Martin, O Sheils, JJ O'Leary. Trinity College Dublin, Dublin, Ireland.

Background: Ovarian cancer is the leading cause of death from gynaecological malignancy in the Western world. This is in part due to tumours which become chemoresistant. There are many causes of chemoresistance, including hypoxia. Hypoxia is characterised as a low level of oxygen tension within tumours. It induces expression of genes involved in chemoresistance mainly via HIF1α. We wanted to investigate the genetic changes induced by hypoxia in an ovarian cancer model, and determine which genes were likely to contribute to chemoresistance. To do this we first compared gene expression between a parent cell line and its daughter chemoresistant line. We subsequently compared these changes to those induced in the parent cell line when it was exposed to hypoxia.

Design: Two ovarian cancer cell lines, A2780 (cisplatin sensitive) and A2780cis (cisplatin resistant) were grown either in normal oxygen conditions (21%O_2) or in hypoxia (5%O_2) for 72 hours. Total RNA was extracted and run on Affymetrix Human Gene arrays. Data was analysed using X-Ray software (Biotique Systems) and the DAVID functional annotation tool. Genes with a fold-change >2 and with an FDR <0.05 were determined significant.

Results: 1026 genes were altered in A2780cis compared to A2780 cells. Of these, 46 genes were also dysregulated in A2780s when exposed to hypoxia. 29 genes were downregulated in both A2780cis and hypoxic A2780s. These included genes whose suppression is involved in tumorigenesis such as CTH as well as genes with putative tumor suppressor function such as FOXO1, HECA and TXNIP. Expression of genes specifically linked to chemoresistance such as PLK2 were also reduced by hypoxia.

Conclusions: Identification of genes which are involved in both the hypoxic response as well as an induced chemoresistant phenotype sheds light on how chemoresistance is being induced via hypoxia. Interestingly, most of the shared expression changes were downregulation of genes. This may be due to repressor functions of HIF1α or other methods of gene downregulation such as methylation. Identification of these genes may provide novel targets for gene therapy in ovarian cancer patients.

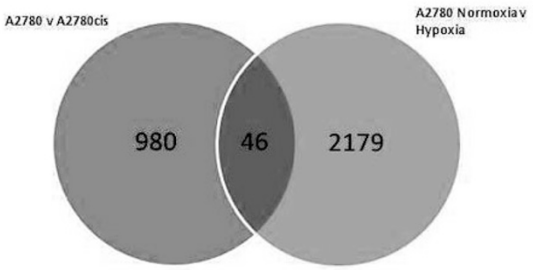

1896 ProtAnalyzer: A Customizable Software for Prediction of Kinase Targets in the Complete Proteome

C Montemayor, E Villegas, J Rosen. University of Wisconsin Hospital and Clinics, Madison, WI; Baylor College of Medicine, Houston, TX.

Background: Tools for proteome-wide identification of kinase targets are necessary for the development of new pharmacologic approaches. *In silico* analyses offer a quick, inexpensive screen that allows the targeted design of validation experiments. Hidden Markov Models (HMM) are robust Bayesian statistical tools widely-employed for DNA and protein pattern recognition. We have created ProtAnalyzer, a customizable HMM-based software, and demonstrate its use by predicting novel Polo kinase 2 (Plk2) phosphorylation targets. Plk2 is a candidate tumor suppressor in triple-negative breast cancer, a disease with poor prognosis for which no targeted therapy exists at present. The discovery of Plk2 substrates is a crucial step to identify potential pharmacologic targets to treat this disease.

Design: ProtAnalyzer runs in any desktop computer. It employs the Viterbi algorithm to search for matches to a user-defined HMM in any number of protein sequences, at

a specified stringency level (*j*). Thus, the universe of emission states encompasses all 20 aminoacids, and the number of transitions is unlimited. To model Plk2 substrates, we constructed an HMM based on the known Plk2 mechanism of action. Targets of this kinase must dock at Plk2's Polo-binding domains (PBDs), and are subsequently phosphorylated in a Ser/Thr residue within a specific aminoacid context. Published consensus sequences for both PBD-binding and Plk2-phosphorylation domains were employed to model an HMM that allows for detection of both motifs at flexible locations and distances within the protein. The *j* value for optimal sensitivity and specificity was determined by running iterations using the published Plk2 substrates as positive controls, as well as with experimentally-validated negative controls and with equivalent but random-generated sequences.
Results: The human proteome was analyzed at a *j* value of 0.001, yielding a list of candidate Plk2 targets, along with the exact location of their phosphorylation and PBD-binding sites. Experiments to validate these targets *in vitro* by bimolecular fluorescence complementation and *in vivo* using Plk2-/- mouse tissue are underway.
Conclusions: ProtAnalyzer is based on HMM principles and can be easily customized to scan entire proteomes for any kind of flexible aminoacid pattern. The list of Plk2 targets obtained from this demonstration represent possible new pharmacologic targets to treat triple-negative breast cancer.

1897 Identification of Circulating Autoantibodies as Novel Ovarian Cancer Biomarkers

MA Murphy, DJ O'Connell, JK O'Brien, S O'Toole, SL O'Kane, C Martin, O Sheils, JJ O'Leary, DJ Cahill. Trinity College Dublin, Dublin, Ireland; University College Dublin, Dublin, Ireland.
Background: Early diagnosis of ovarian cancer (OC) is the most important determinant of survival. However, symptoms of OC are non-specific and there are no reliable biomarkers resulting in the majority of OC diagnosed at late stage. Autoantibodies are an extremely attractive biomarker entity as they are present in blood and easily adapted into current diagnostic platforms. (E.L.I.S.A.) This research aims to determine the utility of autoantibodies as novel OC biomarkers.
Design: Study approval was obtained from SJH/AMNCH research ethics committee. To profile the autoantibody response in patients two different array platforms were used; the Human Expression Library (hEx1) and the Invitrogen Protoarray (n=>10,000 proteins). Benign ovarian disease, early stage ovarian cancer and late stage ovarian cancer patient sera, in addition to Non-Remarkable (Healthy) control subjects were screened. Antigens identified to be associated with these cohorts were interrogated by Western immunoblotting and E.L.I.S.A. Pathway analysis was also performed to identify pathway deregulation associated with malignancy.
Results: Autoantibodies to p53 were identified in patient sera. Western blotting confirmed highly specific OC association, present in 25% (n= 5/25) of late stage OC sera and not present in healthy control sera (n=15). In addition novel autoantigens were identified by both array screening platforms, including a kinase involved in cell adhesion and migration, proteins associated with endocytic and exocytic machinery, a component of the COP9 signalosome complex, a transcriptional repressor and an inhibitory subunit of a nuclear protein phosphatase. Preliminary validation data of these antigens will be presented. Over-represented pathways associated with late stage ovarian cancer were the VEGF signalling pathway and the EGFR1 signalling pathway.
Conclusions: Protein array platforms can be used to identify autoantibody profiles in OC sera. Autoantibodies to p53 were confirmed in 25% of late stage OC patients in line with published data. Pathway analysis performed on antigens identified by autoantibody screening indicated that classical cancer pathways may be deregulated. This indicates that autoantibody profiles detect malignancy associated protein pathway deregulation.
The authors gratefully acknowledge grant support from the Emer Casey Foundation and the clinical contributions of Noreen Gleeson, Tom D'Arcy, Alex Laios, Katherine Astbury and Eamonn McGuinness.

1898 Diagnostic Value of DNA Mutational Analysis of Residual Liquid Gynecologic Cytology in Detecting Malignancy

S Patel, AR Smith, A Mohanty, U Krishnamurti, C Binkert, B Ujevich, SJ Bokhari, JF Silverman, SD Finklestein, Y Liu. Allegheny General Hospital, Pittsburgh, PA; RedPath Integrated Pathology, Inc., Pittsburgh, PA.
Background: Liquid based, monolayer cytology analysis has become the most common approach to manage cervical scrapings and is increasingly applied to other organ specimens. Ancillary molecular mutation testing for cancer-associated changes can be especially useful in these situations. In this study, we investigated the diagnostic utility of DNA mutation analysis from free DNA in the residual gynecological sample fluid that is otherwise not currently utilized.
Design: Cervical scrape specimens were used in this assessment of mutational analysis. Unused residual liquid cytology fluid containing the cellular scraping was centrifuged to create two molecular substrates: 1) cell pellet and 2) cell-free supernatant. DNA was extracted from the cell pellet and 2 ml of the cytocentrifugation supernatant fluid after which mutational analysis was performed by means of PCR/capillary electrophoresis for a broad panel of markers (microsatellite fragment analysis for loss of heterogeneity [LOH] of 16 markers at 19, 3p, 5q, 9p, 10q, 17p, 17q, 21q, 22q). The level and amplifiability of extracted DNA and individual sample mutational profiles were established and compared.
Results: Despite the absence of cells, the cell free component of residual liquid cytology fluid contained abundant (6.7-46.3 ng/ul), amplifiable (Ct less than 30 cycles) DNA suitable for mutation detection and characterization. The benign specimens showed no LOH mutations for the marker panel in either the cellular pellet or the cell free supernatant fluid. The cancer specimen showed extensive loss of heterozygosity mutational change that was highly concordant between the cell pellet sample and the free DNA portion of the specimen. The degree of allelic imbalance was higher in the free DNA sample than the cell pellet indicating greater presence of neoplastic DNA in that compartment compared to the cell pellet.
Conclusions: Our results indicated that DNA molecular mutation analysis on gynecologic fluid can be integrated to a more fully complement liquid based, monolayer cytology practice by utilizing a part of the specimen that is not currently utilized.

1899 Identification of Microvascular Invasion Biomarkers in Hepatocellular Carcinomas by MALDI Imaging Mass Spectrometry

N Pote, T Alexandrov, S Laouirem, J Belghiti, P Bedossa, V Paradis. Beaujon Hospital, Assistance Publique-Hôpitaux de Paris, Clichy, France; INSERM U773, Beaujon Hospital, Clichy, France; University of Bremen, Bremen, Germany; University Denis Diderot, Paris, France.
Background: Microvascular invasion (mVI), a major predictive factor of post-operative tumoral recurrence in patients with hepatocellular carcinoma (HCC), is only detectable after surgery on histological examination of the surgical specimen. So far, there is no reliable biomarker to predict the presence of mVI prior to surgical procedures. MALDI Imaging Mass Spectrometry (IMS) represents a new analytical tool to directly provide the relative abundance and spatial distribution of the whole proteins expressed in a tissue section. The aim of this study was to compare, using MALDI IMS, the tissue proteome of HCC without and with mVI in order to identify biomarkers of mVI.
Design: A total of 56 HCC from various etiologies obtained from surgical specimen, for which clinicopathological data and frozen samples were available, were retrospectively collected. All patients were cirrhotics, and none of them received any neo-adjuvant treatment. After histological examination, two groups of tumors were defined (26 HCC without mVI; 30 HCC with mVI). Cryosectioning was done to yield tissue sections analysed by a pathologist to determine tissue morphology and mirror sections for MALDI IMS. A statistical comparative analysis, using a cross classification model, was then performed in order to identify protein peaks differentially expressed between both groups.
Results: 24 discriminant protein peaks were differentially expressed between both groups, of which 11 were discriminant in more than 30/56 cross classifications. 2 peaks increased in HCC without mVI, whereas 22 increased in HCC with mVI. The latter, which could be used as tissue mVI biomarkers, are under selection for protein characterization. Tissue distribution analysis of the two most discriminant peaks (*m/z* 10,042 and 8,904) showed that *m/z* 10,042 was preferentially expressed in tumor cells, whereas *m/z* 8,904 was overexpressed in the stroma. Interestingly, we have previously described *m/z* 8,904 as a serum biomarker of HCC (Paradis et al., Hepatology 2005).
Conclusions: These results highlight the potential of MALDI IMS to uncover new biomarkers in liver carcinogenesis, and to allow their tissue localization. The identification of mVI biomarkers would be helpful in the therapeutic strategy of patients with HCC.

1900 Molecular and Clinicopathologic Characteristics of HER2 Mutant Lung Adenocarcinoma (ADC)

S Roy Chowdhuri, J Chaft, K Nafa, M Kris, M Zakowski, M Ladanyi, M Arcila. Memorial Sloan-Kettering Cancer Center, New York.
Background: Activating mutations within the tyrosine kinase domain of the *ERBB2*/*HER2* gene have been previously reported in a small subset of lung ADCs. Amplification of HER2 has also been reported in some mutant cases. *HER2* mutations are mutually exclusive with *EGFR* and *KRAS* mutations and are associated with increased sensitivity to specific kinase inhibitors in preclinical models. Previous studies have been mainly carried out on East Asian patients. The frequency and clinicopathologic characteristics of *HER2* mutations and amplification have not been defined in the US population.
Design: Consecutive clinical cases of lung ADC (n=501) known to be negative for mutations in *EGFR* (exons 18-21) and *KRAS* exons 2 (codons 12-13) and 3 (codon 61) were selected based on DNA availability. *HER2* mutation analysis was done by fragment analysis for small indels in exon 20. A subset of tumors was tested for *ALK* fusions and for HER2 amplification by FISH.
Results: *HER2* mutations were present in 5% (25/501) of EGFR neg / KRAS neg lung ADCs. Twenty-four (96%) were exon 20 insertions and 1 (4%) was a point mutation (L755S). None of the 23 *HER2*-mutants tested for an *ALK* fusion by FISH were positive. HER2 amplification was not detected in any of the 10 mutant cases tested. The incidence of *HER2* mutations in the "triple negative" (*EGFR/KRAS/ALK*) group was 7.6% (23/303). Morphologically, 84% (21/25) were mixed ADCs moderately or poorly differentiated. One tumor was well differentiated and 3 could not be graded due to small sampling but had high grade morphology. Eight tumors had a bronchoalveolar component and 2 had a mucinous component.
The patients (68% female) had a median age of 64 at diagnosis (range 41-87); 13 patients presented with advanced disease; 17 patients were never smokers. The prevalence of *HER2* mutations was significantly higher ($p<0.0001$) in never smokers (15.9%; 17/107) than in current/former smokers (2.2%; 8/369) but there was no significant difference between females (6.5%; 17/260) and males (8/216; 3.7%).
Conclusions: *HER2* mutations in lung ADCs are mutually exclusive with *EGFR* and *KRAS* mutations as well as *ALK* fusions. Compared to EGFR mutant ADC's, *HER2* mutant tumors are morphologically highly heterogeneous with moderate to poor differentiation. While the overall prevalence of these mutations is low, estimated at 2.2% of all lung ADCs, testing of "triple negative" patients identifies *HER2* mutations in 7.6%, thereby more efficiently screening for this subset of patients who could potentially benefit from alternate targeted therapies.

1901 A Novel microRNA-Based Test Demonstrate above 90% Accuracy in Classification of Metastatic Tumors from Patients Diagnosed with Carcinoma of Unknown Primary

M Sanden, G Pentheroudakis, B St. Cyr, A Goussia, D Lebanony, K Stoyianni, A Faerman, G Fountzilas, L Cohen, V Malamou-Mitsi, N Pavlidis. Rosetta Genomics Inc., Philadelphia, PA; Ioannina University Hospital, Ioannina, Greece; Rosetta Genomics Ltd., Rehovot, Israel; Hellenic Cooperative Oncology Group, Athens, Greece.

Background: Identification of the tissue of origin of metastatic tumor is vital to its management. Carcinoma of unknown primary (CUP) is common in oncology, representing 3-5% of all invasive malignancies. A microarray-based test that measures the expression of 64 microRNAs was employed to identify the tissue of origin of metastatic tumors of CUP cases.

Design: A cohort of resected metastatic lesions from patients diagnosed with CUP was studied. The cohort included 93 samples (from 92 patients) with adequate tissue sample needed for the test. Eight samples failed due to inadequate RNA quality; 85 samples (84 patients) were processed successfully. Test results were compared with clinical presentation including imaging, pathological data (histology and IHC) and therapeutic response.

Results: In this blinded study, the test results were fully concordant with the diagnosis based on all the clinical and pathological information available including follow-up and outcome data in over 90% of the cases. The microRNA test assigned a single putative tissue of origin for 50 samples and two tissues of origin in 34 patients with the first being the more likely diagnosis. When comparing only the first (or single) diagnosis, a concordant level of >83% is achieved. The diagnosis based on the clinical and pathological data that was available at presentation and without additional data gathered throughout patient management had only 70% agreement with the test results. Additional clinical and pathological analysis of the CUP cases is currently ongoing.

Conclusions: In a cohort of metastases from CUP patients, a previously developed test based on the expression profile of 64 microRNAs allowed accurate identification of tissue of origin in the vast majority of the cases. The high accuracy of this test in identifying the tissue of origin of metastasis of unknown primary has been validated by this study and demonstrates its clinical utility. The high concordance of the test results to the final diagnosis of the patient demonstrates the importance of the test to yield additional data valuable for patient's management at an early stage of patient's journey.

1902 Functional Correlates of Jab1 Networks in Triple Negative Breast Cancer

MM Sasamoto, TT Vu, FX Claret, ME Edgerton. UT MD Anderson Cancer Center, Houston, TX.

Background: Jab1 (c-Jun activation domain-binding protein 1) (also know as COPS5/CSN5) has been demonstrated to cause low levels of p27, a cell cycle checkpoint, thus promoting proliferative behavior. Aberrant expression has been reported in metastatic breast cancer compared with low or absent levels in normal breast tissue. We have found that Jab1 mRNA is elevated in approximately 50% of triple negative breast cancer (TNBC) patients, indicating a possible role for regulation of Jab1 as a therapy in TNBC. We present results from a study of gene expression patterns associated with Jab1 in TNBC.

Design: Using Backward Chaining Rule Induction (BCRI), a network inference strategy that we introduced previously, we identify other agents associated with JAB1 activity in TNBC. BCRI was applied in a cohort of 99 patients compiled from the literature. We examined the persistence of thee relationships in The Cancer Genome Atlas (TCGA) data, and reviewed the annotation and known relationships between Jab1 and these other genes.

Results: High levels of RRS1, TGS1, C8orf33, SIAHBP1, HSF1, and EXOSC4 predict high levels of Jab1 in the TNBC data. The TCGA data only contains only RRS1 and TGS1, which maintain a correlation with Jab1. RRS1 is involved in spindle organization, while TGS1, C8orf33, SIAHBP1, and EXOC4 play a role in mRNA processing. The relationship with HSF1 is not clear. HSF1 has been associated with Her2neu activity in breast cancer.

Conclusions: Data mining of TNBC to explore relationships involving Jab1 are important in the development of efforts to target Jab1 as a potential therapy in TNBC and other aggressive breast cancer. We have found some interesting relationships, possibly downstream (RRS1, TGS1, C8orf33, SIAHBP1 and EXOSC4) and another that is possible additive (HSF1).

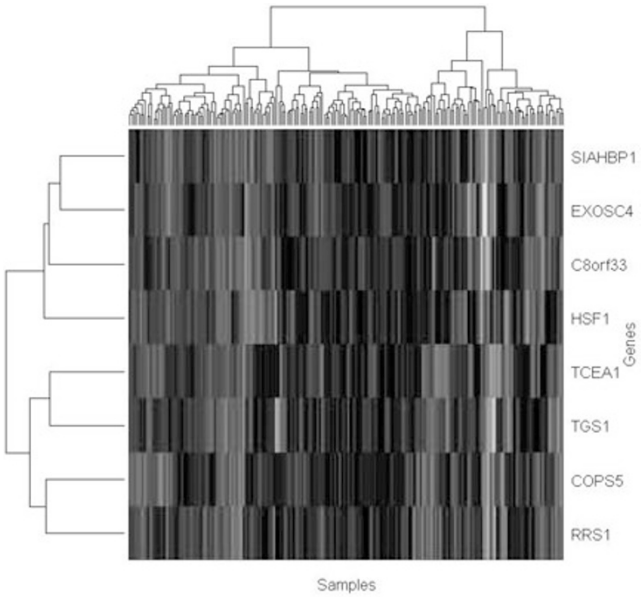

An additive factor might introduce resistance to therapy. These relationships require further study.

1903 CpG Island-Containing *BRCA1* Distal Promoter Is Associated with Breast Stem Cells and Resistance to Doxorubicin

R Shen, W Zhou, Z Peng, M Teng, Y Liu, A Toland, K-Y Teng, JR Chao, S Liu, M Wicha, H-JL Lin. The Ohio State University, Columbus, OH; Indiana University, Indianapolis, IN; University of Arizona, Phoenix, AZ.

Background: Multiple lines of evidence have implicated the existence of somatic normal and cancer stem cells but little is known about the underlying mechanisms.

Design: Cancer stem cells were obtained from SUM159 cells by capturing subpopulation displaying elevated ALDH1 using ALDEFLUOR assay. Afterwards, MBD-seq (Methyl-binding domain sequencing) method was implemented to seek stem cell-associated key regulators controlled by DNA methylation in a genome-wide scale, among which *BRCA1* ranked of the greatest interest. Thus combined bisulfite restriction analysis (COBRA) and quantitative DNA methylation MassARRAY were applied to confirm methylation levels of *BRCA1* in various cell contexts. Finally, *in vitro* DNA methylation followed by luciferase assay was used to assess promoter activity of regions flanking *BRCA1* promoter and its response to DNA methylation.

Results: We demonstrated that an unreported distal promoter region of *BRCA1* was hypermethylated in ALDH1+ SUM159 cells, which was confirmed in other breast cancer cell lines, nonmalignant breast tissues and a xenografted breast tumor. Moreover, this region was validated to bear promoter activity comparable to the previously reported *BRCA1* proximal promoter, which was sensitive to DNA methylation. While the latter was reported to be infrequently methylated in breast tumors, its methylation was undetectable in this study. Conversely, methylation at this novel distal promoter occurred in all 16 primary tumors we tested with 6 of which displayed a positive relationship between levels of ALDH1 and methylation of *BRCA1*. It was further proven by inverse staining pattern of BRCA1 and ALDH1 in immunohistochemistry. Surprisingly, methylation at this promoter was also elevated in survivor cells after a treatment with chemotherapeutic agent Doxorubicin, but not with Placitaxel, causing gene suppression.

Conclusions: Our findings unveiled that hypermethylation at a novel *BRCA1* promoter might epigenetically regulate cancer stem-like cell population and cell resistance to Doxorubicin.

1904 Stemness Gene Expression Profiles in Cancer Stem Cell Progenies Derived from a Cell Line Panel +/- BRAF Mutation

G Sommerville, P Smyth, JJ O'Leary, O Sheils. Trinity College Dublin, Dublin, Ireland.

Background: BRAF mutation is implicated in up to 8% of all solid tumours and so represents an important target for therapeutic intervention. The V600E BRAF mutation confers constitutive kinase activity, independent of mitogen initiation, within the MAPK-ERK pathway leading to aberrant cell signalling.

Cancer stem cells are reputed to exist in many human cancers. They possess characteristics similar to normal human stem cells and are believed to contribute to disease aggressiveness, metastasis and chemoresistance through their capacity for self-renewal and differentiation.

This project sought to derive stem cell holoclones from various different cancer cell lines, (BRAF ^{WT} & ^{MUT}), to determine if they have stemness characteristics and to compare their expression profiles.

Design: Established melanoma, thyroid, ovarian and colon cancer cell lines were used in this study. BRAF status was determined using a modified SNP-allelic discrimination TaqMan assay. Parental cells were plated at low density onto high salt agar to positively select for holoclone formation. RNA was extracted from parental cells and derived holoclones. TaqMan RT-PCR was employed to investigate stemness gene expression profiles of holoclones relative to parental cells. The targets examined were:

NANOG -Stem cell proliferation and self-renewal
Oct4 -Stem cell pluripotency
SNAIL2 -Epithelial Mesenchymal Transition
Sonic hedgehog homolog (Shh) -Stem cell proliferation control
TGF-β -TGF pathway ligand
CDKNIB -Endogenous control
Expression of NANOG protein was assessed by immunoflouresence with Confocal Microscopy.
Results: Each holoclone displayed upregulation of at least 2 stemness genes compared to parent cells. NANOG; involved in self-renewal, was the most consistently upregulated marker of all holoclones analyzed. Melanoma cell lines (^{WT} & ^{MUT}) had upregulation of each target analysed.
NANOG protein expression was significantly increased in holoclones compared to parental cells, was localised to the apical side and cell surface -a pattern also seen in ES cells and putative cancer stem cells.
After holoclone harvesting, plates were maintained. New holoclones consistently grew at the precise locations previously harvested, implying a strong capacity for self-renewal.
Conclusions: We present evidence that cancer stem cells can be consistently derived from established cell lines. These cells possess characteristics similar to normal human stem cells as displayed by gene expression profiling and immunofluoresence. We also observed capacity for self-renewal in these cancer cell supopulations.

1905 A Comparison of Targeted Next Generation Sequencing from Paired Formalin-Fixed and Fresh Frozen Specimens

DH Spencer, E Duncavage, RD Mitra, S Kulkarni, K Seibert, R Nagarajan, MA Watson, JD Pfeifer. Washington University, St. Louis, MO.
Background: Next-generation sequencing (NGS) has the potential to revolutionize molecular testing of cancer through comprehensive, unbiased, and inexpensive mutation detection. However, for these methods to be practical they must be robust to a diversity of specimen types, including formalin-fixed diagnostic tissue. We evaluated the performance and quality of targeted NGS in a series of paired formalin-fixed and fresh-frozen tissue to determine if formalin-fixed tissue is an adequate substrate for these platforms.
Design: Sequence data were generated for 15 pairs (30 specimens total) of case-matched fresh-frozen and formalin-fixed lung adenocarcinoma specimens. Indexed sequencing libraries were prepared with 1ug of DNA that passed ladder amplification and spectrophotometry quality-control assessment. Enrichment for 28 target genes was performed with custom capture reagents and enriched libraries were sequenced by multiplex sequencing. Variants were identified from mapped reads using a custom pipeline based on the Genome Analysis Toolkit. Read quality metrics and single-nucleotide variant calls were compared between sample types. For a subset of cases, calls from sample pairs were compared to previously-generated array-based genotype data.
Results: Multiplex sequencing produced 2,000-10,000-fold coverage of the target region across all samples. There were small, but statistically-significant differences in insert size (179 bp (fixed) vs 225 bp (frozen); $P<10^{-7}$), aligned bases per read (96 bp (fixed) vs. 98 bp (frozen); $P<10^{-5}$), and the fraction of unique reads (22% (fixed) vs 31% (frozen); $P<10^{-3}$). However, the mean number of high-quality bases per read, mean error rate, and proportion of positions with high-quality basecalls were not significantly different. Basecall concordance between paired samples was >99.99%, with an average of only 5 discordant positions over the ~300 kilobase-pair target interval per case. The concordance between basecalls and array-based genotypes was >98% for each specimen type.
Conclusions: We have shown that next-generation sequencing using DNA from formalin-fixed specimens yields comprehensive and accurate sequence information that is comparable to that from fresh-frozen tissue. These results indicate that NGS technology can be readily integrated into the standard surgical pathology workflow and demonstrate the feasibility of large-scale sequencing of formalin-fixed surgical pathology specimens for basic science, translational research, and clinical trials.

1906 Exome Sequencing and Integrative Mutational Profiling of Lethal Castrate Resistant Prostate Cancer

SA Tomlins, CS Grasso, DR Robinson, Y-M Wu, S Dhanasekaran, MJ Quist, X Cao, X Jing, JC Brenner, DR Rhodes, KJ Pienta, AM Chinnaiyan. Michigan Center for Translational Pathology, University of Michigan Medical School, Ann Arbor, MI; Compendia Biosciences and University of Michigan Medical School, Ann Arbor, MI.
Background: Characterization of the prostate cancer transcriptome and genome has identified chromosomal rearrangements and copy number gains/losses, including ETS gene fusions, *PTEN* loss and *AR* amplification, that drive prostate cancer development and progression to lethal metastatic castrate resistant prostate cancer (CRPC). As less is known about the role of mutations, we sequenced the exomes of 21 lethal CRPCs (including three different foci from the same patient) and 3 localized prostate cancers.
Design: Exome libraries were generated from matched tumor/normal DNA pairs and sequenced with the Illumina GAII Genome Analyzer or the Illumina HiSeq in paired end mode. Results were integrated with a compendium of related genomic data, including a novel large matched gene expression/aCGH data set.
Results: Exome sequencing demonstrated low overall mutation rates even in heavily treated CRPC (2.23/Mb) and confirmed the monoclonal origin of lethal CRPC. No genes were highly mutated (>50% of cases), however we identified three known (*AR, TP53,* and *ZFHX3)* and two novel genes as significantly mutated in prostate cancer. Through integration with a compendium of related genomic data, we confirm deregulation of genes known to play driving roles in prostate cancer and nominate genes recurrently disrupted, including *GRM1*, *STAG2*, the ETS family member *ETS2* and genes at 5q21 (in ETS fusion$^-$/PTEN deletion$^-$ cancers). Finally, we identified novel recurrent mutations in an *AR* collaborating factor which disrupt androgen signaling and increase proliferation.
Conclusions: Through our integrative analysis, we provide a global description of the mutational landscape of CRPC and prioritize candidates for future study. Updated results on over 40 CRPC will be presented.

1907 Absence of ERG Expression Predicts Early Prostate Cancer Biochemical Recurrence When Combined with DNA Methylation Status of a Development-Associated Gene

D Trudel, K Kron, L Liu, J Trachtenberg, N Fleshner, B Bapat, TH Van der Kwast. Princess Margaret Hospital, University Health Network, Toronto, Canada; Samuel Lunenfeld Research Institute, Mount Sinai Hospital, Toronto, Canada.
Background: Recent work supports interplay between ERG expression secondary to TMPRSS2-ERG fusion and epigenetic changes. Through a genome-wide epigenetic screen, we discovered a development-associated gene (DAG) with high promoter methylation levels in prostate cancer. Our objective was to correlate DAG methylation status with ERG expression and biochemical recurrence-free survival (BRFS) in an independent prostate cancer cohort.
Design: Two-hundred-fifty-eight patients treated by radical prostatectomy between 1998 and 2001 were identified. Macrodissection of tumors was performed prior to quantitative DNA methylation analysis (MethyLight) for DAG promoter. Paraffin-embedded blocks were rearranged in tissue microarrays in order to identify ERG expression in tumors using immunohistochemistry as a surrogate for TMPRSS2-ERG fusion. Univariate BRFS was assessed using the Kaplan-Meier curve and log-rank tests. Cox proportional hazards regression analysis was used for multivariate BRFS.
Results: A total of 219 pT2 to pT4 cases were available for analysis. Median follow-up was 4.67 years. ERG expression was found in 51% of the cases. DAG methylation was significantly greater in tumor specimens compared to benign glands and was greater in ERG positive cases (p-values < 0.001). Univariate analysis showed no association between DAG methylation or ERG expression and BRFS. Patients with ERG negative/high DAG methylation tumors however had shorter BRFS. Furthermore, in a multivariate model that included clinicopathological data, absence of ERG expression and high methylation of DAG were both significant predictors of recurrence (p-values 0.03 and 0.04, respectively).
Conclusions: Although TMPRSS2-ERG fusion is identified in approximately 50% of prostate cancer, there is conflicting evidence regarding its prognostic value in the literature. We show that (1) ERG expression is associated with increased methylation of DAG promoter and (2) patients with tumors diverging from this profile, i.e. with high methylation of DAG promoter in the absence of ERG expression have shorter BRFS. These results suggest that TMPRSS2-ERG fusion is associated with methylation levels of specific genes, and also add prognostic value to TMPRSS2-ERG fusion status of prostate cancer.

1908 Prolonged Room Temperature Ischemia Does Not Affect the Quality of Total Tissue RNA

L True, B Nghiem, B Lakely, C Morrissey. University of Washington, Seattle.
Background: Molecular assays provide guidance for identifying tumors likely to respond to targeted therapy. Many of these assays require high quality RNA. A method widely used to assess RNA quality uses the Bioanalyzer (Agilent). Degree of RNA integrity is reported as RNA Integrity Numbers (RIN), using a Bioanalyzer. RINs range from 1 to 10 (1 indicates degradation of total RNA; 10 indicates little or no RNA degradation). We hypothesized that the length of time a samples sits at room temperature before freezing (the cold ischemia time) correlates with extent of RNA degradation.
Design: Prostate cancer and benign tissues were acquired from both rapid autopsy (RA; n=35) and radical prostatectomy (RP; n=72) samples. Cold ischemia times were recorded. Integrity of total RNA extracted from tissue aliquots was determined on an Agilent 2100 Bioanalyzer.
Results: RINs of RP samples (range of cold ischemia time: 20 to 100 min.) ranged from 2.4 to 9.7. There was no correlation of RIN with time.

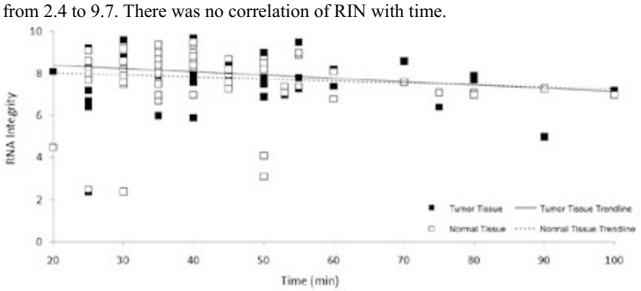

RINs of RA samples (range of time from patient death to tissue stabilization by freezing: 2 to 6.5 hrs.) ranged from 3.0 to 7.9 (Different samples from each autopsy differed in RIN).

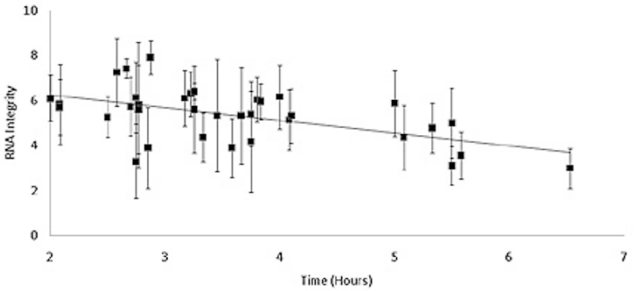

With several exceptions, there was a trend toward decreasing RIN with time, though some samples after 5 hours of cold ischemia still had a RIN of 7.

Conclusions: Despite prolonged cold ischemia times (up to 2 hrs for RP samples and 6.5 hrs. for RA samples), the quality of RNA does not significantly decrease in a time-dependent manner. Pre-analytical factors, i.e. warm ischemia time, hypoxia, high protein pre-op diet, etc., are known to affect levels of specific mRNA's. Since the quality of total RNA was essentially independent of cold ischemia time, we cannot rely upon the RIN to reflect the effect of cold ischemia time on RNA quality for tissue acquired within 7 hours of devitalization. To predict which tissue samples have high quality RNA, a better assay of RNA integrity is needed.

1909 MiR-335 Is Upregulated upon Retinoic Acid-Induced Differentiation of NTera-2 Human Embryonal Carcinoma Cell Line and Can Induce Differentiation

S Vencken, M Gallagher, S Elbaruni, C Martin, O Sheils, J O'Leary. Trinity College Dublin, Dublin, Ireland.

Background: MicroRNAs (miRNAs) are endogenous, non-coding RNA molecules of 22-25 nucleotides in length and regulate various cell processes, by inhibiting mRNA translation.

NTera-2 embryonal carcinoma cells are frequently used to study both cancer stem cells (CSCs) and human embryonal stem cells (hESCs).

Like hESCs and many CSC types, NTera-2 cells are sensitive to all trans retinoic acid (ATRA) –induced differentiation. Upon subjecting these cells to ATRA, phenotypic change in cell morphology, a reduction in core stem cell markers and an increase in differentiation markers have been shown shortly after by various laboratories, including ours.

Design: Our study showed a wide range of differential miRNA expression upon incubation of NTera-2 cells in 10^{-5} M ATRA in growth medium for 72 hours. Hsa-miR-335 was among some of the most substantially upregulated miRNAs upon ATRA-induced differentiation of NTera-2 cells.

The highly cited miRNA target prediction software packages, TargetScan 5.1 and miRANDA, predict miR-335 binding regions within the 3' untranslated regions of various CSCMs, among which OCT3/4 and SOX2.

We proceeded to upregulate this miR-335 in NTera-2 cells by transfecting Ambion's Pre-miR miRNA precursors, stable mimics of endogenous miRNAs. As a negative control, we used the manufacturer's Pre-miR Negative Control #1, a scrambled, non-targeting Pre-miR.

Results: Results showed a clear morphological change in the NTera-2 cells after four days, with characteristics of cell differentiation and cell senescence. Cell viability studies using an MTT assay showed a significant reduction in cell proliferation.

Gene expression analysis with qRT-PCR showed a significant downregulation of OCT3/4 and NANOG CSCMs. SOX2, another CSCM frequently associated with the previous two, was significantly upregulated at the gene level, but this was not beyond the margin considered to be biologically insignificant. Protein expression analysis with Western blot showed a significant downregulation of OCT3/4 and SOX2, the latter result suggesting post-transcriptional intervention of the SOX2 mRNA, possibly by miRNA.

Conclusions: Our findings suggest miR-335 to be a miRNA involved in key regulatory mechanisms during early differentiation in NTera-2 cells. We are currently focused on validating predicted targets of miR-335 we believe are crucial to the maintenance of the pluripotent and self-renewal state.

1910 Salinomycin: Antitumoral Effects and Gene Expression in Neuroblastoma Cells

P Weerasinghe, ML Buja, RE Brown. UT Health Medical School, Houston, TX.

Background: *Salinomycin*, an anticoccidial agent used in the poultry industry, has recently been identified as an anticancer stem cell agent by high-throughput screening and shown to have efficacy against breast cancer stem cells.

Design: This study was designed to assess the involvement of molecular cell death pathways in salinomycin-treated human neuroblastoma (SK-N-A-S) cells. Preliminary results indicated that salinomycin was capable of inducing apoptosis and autophagy in neuroblastoma cells.

Results: Dose-response studies, followed by TUNEL and LC3 assays confirming apoptosis and autophagy respectively, indicated that salinomycin at concentratrations of 5 μM for 24 hours induced apoptotic and autophagic cell death. High density oligonucleotide microarray analysis and validation by *q RT-PCR* of salinomycin-induced apoptosis and autophagy showed an increased expression of cell death-related genes at 12 hours of drug exposure. Furthermore, direct comparison of expression patterns showed 158 apoptosis-related genes versus 19 autophagy-related genes.

Conclusions: These data suggest that salinomycin might be affecting signaling of apoptosis- and autophagy-related genes with a preponderance of known apoptosis genes. Also the high number of probes altered suggests the involvement of multiple signaling pathways during salinomycin treatment. The increase in the number of probes altered at the 12 and 24 hour time points suggest more widespread cellular activation, including survival and death signaling, at longer exposures in this human neuroblastoma cell line.

1911 Whole Exome Sequencing of Both Components of a Mixed Adenocarcinoma/Small Cell Carcinoma of the Gallbladder

LD Wood, Y Jiao, A Maitra, P Argani, JL Cameron, N Papadopoulos, KW Kinzler, B Vogelstein, RH Hruban. Johns Hopkins University School of Medicine, Baltimore, MD.

Background: Each year 7,200 Americans are diagnosed with cancer of the biliary tract, and each year 3,600 die from their disease. While the majority of carcinomas of the gallbladder are adenocarcinomas, rare mixed adenocarcinoma/small cell carcinomas occur. The molecular genetic alterations underlying the development of these neoplasms are poorly understood.

Design: Each component of a fresh-frozen mixed adenocarcinoma/small cell carcinoma of the gallbladder was macrodissected to achieve a neoplastic cellularity of >70%. Each neoplastic component, as well as normal tissue from the same patient, was analyzed by whole exome sequencing using next-generation sequencing technology. Known SNPs were removed from the analysis, and the alterations in the two components of the neoplasm were compared to the patient's normal sequence to identify somatic (tumor-specific) mutations.

Results: Somatic mutations were identified in a total of 55 genes. Interestingly, the majority of the somatic mutations (35) were shared between both components, including mutations in the tumor suppressor gene *TP53* as well as several mutations with predicted functional consequences, such as a nonsense mutation in the ephrin receptor *EPHA1* and a frameshift mutation in transmembrane serine protease *TMPRSS7*. Somatic mutations unique to each morphologic component were also identified. Nine mutations occurred only in the small cell carcinoma, including a nonsense mutation in the GTPase activator *ARHGAP28*, while the adenocarcinoma possessed 11 unique mutations.

Conclusions: Whole exome sequencing can be used to define the genesis of mixed neoplasms. In this mixed adenocarcinoma/small cell carincoma of the gallbladder, the majority of the somatic mutations were shared between the two components, but unique somatic mutations were also identified in both the adenocaricoma and small cell carcinoma. This suggests a clonal origin followed by divergent genetic changes which subsequently contributed to the distinct morphologies of the two components.

1912 Alignment in a SNAP: Cancer Diagnosis in the Genomic Age

M Zaharia, B Bolosky, K Curtis, D Patterson, A Fox, D Patterson, S Shenker, I Stoica, T Sittler. UCSF, San Francisco, CA; UC Berkeley, Berkeley, CA; Microsoft, Redmond, WA.

Background: As the cost of DNA sequencing continues to drop at a pace exceeding that of Moore's Law, there is growing need for tools that can efficiently analyze ever larger bodies of sequence data. By mid-2013, it is estimated that we will reach the $1000 genome. The cost of sequencing a person's genome will then enter the realm of routine clinical practice and it is expected that each cancer patient will have their genome and their cancer's genome sequenced. In order to assemble and interpret this information from the massive numbers of short reads generated by current sequencing machines, significant technological advancement is necessary. Here, we address the first step in the interpretation of a cancer genome from raw sequence information: sequence alignment.

Design: We tested SNAP (Scalable Nucleotide Alignment Package) against the most popular short read aligners, including BWA, Bowtie, and SOAP. Trials included generation of reads from the hg19 build of the human genome with simulated mutations, insertions, and deletions. Additional trials demonstrating superior performance against longer reads and actual whole genome sequencing data sets will be presented at the conference.

Results: SNAP significantly outperforms existing aligners in terms of speed while achieving higher accuracy.

Comparison of Aligners using 125bp Simulated Single End Reads

Aligner	Seconds per Million Reads	Accuracy (%)	False Positive (%)
bowtie*	1966	88	0.07
BWA*	3021	93	0.05
MAQ*	17506	92.7	0.08
SOAP2*	555	91.5	0.17
SNAP	10	94	0.05

* These numbers were previously published in [Li et al. Bioinformatics Vol. 25 no. 14 2009, pages 1754–1760]

Conclusions: Currently, aligning a single genome takes roughly 1000 processor hours. We demonstrate a new algorithm and software package called SNAP, which is capable of aligning a genomic dataset consisting of up to 3 billion 100bp reads in 1 hour on a machine rented from Amazon for $2. This is a 100X improvement over current technologies with greater accuracy, higher error tolerance and better performance on longer read lengths, making the package compatible with upcoming developments in sequencing technology. Additionally, SNAP can align against a consensus of genomes rather than a single sequence, allowing it to more effectively discriminate between hereditary sequence variation and somatic mutations. Using SNAP, we can begin to realize the benefits of large sequencing projects such as the TCGA, and to translate their results into personalized therapeutic recommendations for each patient.